

# Independent circuits in the basal ganglia for the evaluation and selection of actions

Marcus Stephenson-Jones<sup>1,2</sup>, Andreas A. Kardamakis, Brita Robertson, and Sten Grillner<sup>2</sup>

Department of Neuroscience, Karolinska Institutet, SE-171 77 Stockholm, Sweden

Contributed by Sten Grillner, August 8, 2013 (sent for review June 7, 2013)

**The basal ganglia are critical for selecting actions and evaluating their outcome. Although the circuitry for selection is well understood, how these nuclei evaluate the outcome of actions is unknown. Here, we show in lamprey that a separate evaluation circuit, which regulates the habenula-projecting globus pallidus (GPh) neurons, exists within the basal ganglia. The GPh neurons are glutamatergic and can drive the activity of the lateral habenula, which, in turn, provides an indirect inhibitory influence on midbrain dopamine neurons. We show that GPh neurons receive inhibitory input from the striosomal compartment of the striatum. The striosomal input can reduce the excitatory drive to the lateral habenula and, consequently, decrease the inhibition onto the dopaminergic system. Dopaminergic neurons, in turn, provide feedback that inhibits the GPh. In addition, GPh neurons receive direct projections from the pallium (cortex in mammals), which can increase the GPh activity to drive the lateral habenula to increase the inhibition of the neuromodulatory systems. This circuitry, thus, differs markedly from the “direct” and “indirect” pathways that regulate the pallidal (e.g., globus pallidus) output nuclei involved in the control of motion. Our results show that a distinct reward–evaluation circuit exists within the basal ganglia, in parallel to the direct and indirect pathways, which select actions. Our results suggest that these circuits are part of the fundamental blueprint that all vertebrates use to select actions and evaluate their outcome.**

striosomes | reward/aversion | pallium/cortex | evolution

**T**o achieve a goal, animals need to select actions and evaluate their outcome to determine whether their goal was achieved. In mammals, the basal ganglia play a key role in the selection of actions (1–3) and have more recently been suggested to additionally contribute to predicting and evaluating the outcome of the selected actions (4–8).

The so-called “direct” and “indirect” pathways through the basal ganglia are present in all vertebrates and act together to select actions by decreasing tonic inhibition of the basal ganglia output nuclei [globus pallidus interna (GPI) and substantia nigra pars reticulata (SNr)] on a selected motor program and increasing the inhibition onto other competing actions. The output of these selection circuits target brainstem and thalamic motor areas, and neurons within this circuit are modulated by various aspects of movement kinetics related to the initiation and modulation of ongoing actions.

In addition to the output neurons that project to motor areas, a separate subpopulation of pallidal neurons projects to the lateral habenula (9–12), a structure involved in evaluating and predicting the motivational value of actions. Recent *in vivo* recordings in primates have shown that the activity of these habenula-projecting pallidal neurons is modulated by the cues that predict the availability of reward (13, 14) and not by aspects of movements. The majority of these pallidal neurons, as with lateral habenula neurons, are excited in response to errors in reward prediction or in expectation of an adverse outcome (14, 15). In addition, selective activation of this pallido-habenula projection in rodents can induce aversive conditioning (16) and activation of the lateral habenula can devalue a rewarding stimulus

(17). These results show that the pallidal neurons projecting to the habenula encode information about the expected and achieved value of an action.

Consequently, it appears that separate populations of neurons in the globus pallidus are involved in the selection (brainstem/thalamic projecting) and evaluation (habenula-projecting) of actions. This raises the possibility that independent circuits within the basal ganglia control these globus pallidus populations to regulate action selection or evaluation. Although the selection circuitry, as mentioned above, is described in detail, no studies have determined the evaluation circuitry within the basal ganglia that provides the source of the reward-related signals to the habenula-projecting pallidal neurons.

To address this, we analyzed the circuitry regulating the habenula-projecting pallidum in lamprey. In this ancient vertebrate species, the habenula and thalamic/brainstem-projecting pallidal neurons are located in separate, nonoverlapping locations (11, 12), which afford the possibility of untangling the circuitry that influences these separate populations.

Using electrophysiological, tracing, and immunological techniques, we show that the habenula-projecting globus pallidus (GPh) and the GPI are regulated by independent circuits. The direct and indirect pathways control the GPI, as in mammals (11). In contrast, the GPh is not influenced by these pathways but, instead, receives direct excitatory projections from the pallium (cortex), inhibitory input exclusively from striosomal striatal neurons, and inhibitory dopaminergic feedback. Furthermore, we show that in lamprey the GPI and GPh represent two distinct nuclei that differ in the topographic location, neurotransmitter phenotype, molecular expression, electrophysiological properties, and connectivity. Our results show that there are two independent sets of circuits through the basal ganglia, one regulates action selection by controlling the output of the GPI/SNr and another,

## Significance

**The activity in the dopaminergic reward system of the brain is concerned with the evaluation of actions and is controlled from the lateral habenulae, in all vertebrates investigated, from lamprey to primates. This study considers the mechanisms by which the lateral habenulae is controlled. We show here that a particular group of nerve cells conveys excitatory drive to the lateral habenulae, which, in turn, receive excitatory input from pallium (cortex in mammals) and inhibitory control from a specific compartment (striosomes) in the basal ganglia. This control system is critical for value-based decisions, important in all groups of vertebrates.**

Author contributions: M.S.-J. and S.G. designed research; M.S.-J., A.A.K., and B.R. performed research; M.S.-J. and A.A.K. analyzed data; and M.S.-J. and S.G. wrote the paper. The authors declare no conflict of interest.

<sup>1</sup>Present address: Cold Spring Harbor Laboratory, Cold Spring Harbor, NY 11724.

<sup>2</sup>To whom correspondence may be addressed. E-mail: mstephen@cshl.edu or Sten.Grillner@ki.se.

This article contains supporting information online at [www.pnas.org/lookup/suppl/doi:10.1073/pnas.1314815110/-DCSupplemental](http://www.pnas.org/lookup/suppl/doi:10.1073/pnas.1314815110/-DCSupplemental).

which we identify here, regulates the output of the GPh to predict and evaluate the outcome of the selected actions.

## Results

**The GPh Projects Selectively to the Habenula and Is Glutamatergic.** In lamprey, there are two separate populations of pallidal neurons located in topographically distinct nuclei (red and blue in Fig. 1A). Retrograde tracing reveals that pallidal neurons projecting to the habenula are situated in a nucleus, here referred to as the GPh (Fig. 1A–C; cases,  $n = 6$ ) (12). In contrast, pallidal neurons that project to the thalamus and brainstem motor regions are situated more caudally in the lamprey homolog of the GPi/GPe (Fig. 1A) (11, 18, 19). Both the GPi/GPe and GPh receive input from the striatum (Fig. 1D and E) (11, 12).

To determine whether the GPh neurons exert a tonic influence on the habenula, because of spontaneous activity, patch-clamp recordings were made from these neurons. Our results revealed that 70% of the neurons recorded in the GPh, in either whole-cell or on-cell patch configuration displayed spontaneous activity ( $n = 49/67$ ; Fig. 1F and G). Furthermore, eight of nine GPh neurons that had been retrogradely labeled from the habenula were spontaneously active. In on-cell recordings, these neurons fired with instantaneous firing frequencies ranging between 0.2 and 7 Hz, with a mean around 1 Hz ( $n = 19/25$ ). In whole-cell recordings, firing frequencies ranged from 0.25 to 6 Hz ( $n = 30/42$ ). This spontaneous firing of the GPh neurons is driven by intrinsic properties because the firing frequency was not significantly altered by blocking the glutamatergic synaptic input with 40  $\mu\text{M}$  6-cyano-7-nitroquinoxaline-2,3-dione (CNQX) and 50  $\mu\text{M}$  (2R)-amino-5-phosphonovaleric acid (AP5) ( $n = 6$ ; Fig. 1G and H; control,  $1.07 \pm 0.36$ ; CNQX and AP5,  $1.03 \pm 0.31$  Hz).

To determine whether the GPh neurons displayed a distinct neurotransmitter phenotype, we combined immunohistochem-

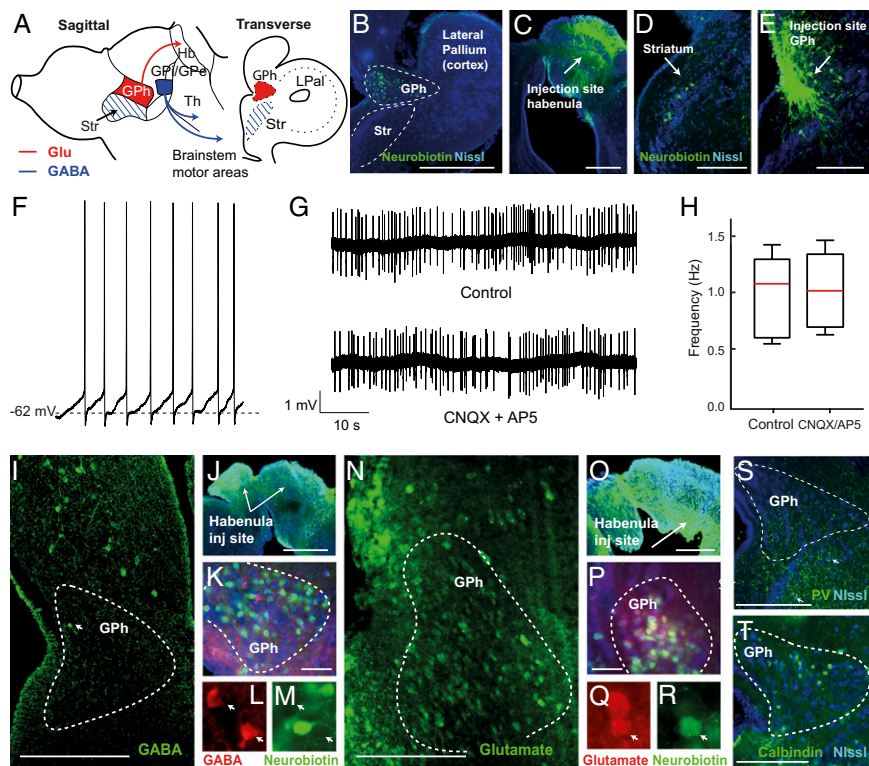
istry with retrograde tracing. In contrast to the GPi/GPe neurons, which we have previously shown are GABAergic (11), our results now show that most GPh neurons express glutamate (Fig. 1N and P) and very few neurons in GPh express GABA (Fig. 1I). Furthermore, none of the GPh neurons retrogradely labeled from the habenula were GABAergic (Fig. 1J–M;  $n = 3$ ), whereas the majority of the retrogradely labeled projection neurons expressed glutamate (Fig. 1O–R; cases,  $n = 4$ ). The GPh and GPi/GPe neurons also differ in their calcium binding-protein expression because immunohistochemistry revealed that, unlike GPi/GPe neurons (11), GPh neurons do not express parvalbumin (Fig. 1S; cases,  $n = 3$ ). In contrast, a population of neurons immunoreactive for calbindin was observed within the GPh (Fig. 1T).

Together, these results show that GPh is a glutamatergic pallidal nucleus that differs from the GABAergic GPi/GPe in its projections, neurotransmitter phenotype, topographic location, and molecular expression. However, both GPh and GPi/GPe neurons (11) are spontaneously active and receive input from the striatum.

## GPh and GPi/GPe Neurons Differ in Their Electrophysiological Properties.

Because the GPh and GPi/GPe neurons differ in their neurotransmitter phenotype and molecular expression and are located in distinct nuclei, we next aimed to determine whether they also differed electrophysiologically. Whole-cell patch-clamp recordings revealed that neurons in both nuclei exhibited spontaneous activity and had linear current–voltage relationships in response to hyperpolarizing current injections (Fig. 2A–C). Furthermore, both types of neuron showed reliable and regular spiking with a limited spike frequency adaptation during sustained current injections (Fig. 2A and B). In contrast, the input resistance, membrane time constant, action potential half-width, and resting membrane potential significantly differed between the GPh

**Fig. 1.** Anatomical and electrophysiological evidence showing that the GPh represents a glutamatergic (Glu) pallidal nucleus. (A) Schematic drawings of sagittal and transverse sections through the lamprey brain, indicating the location of the GPh and the lamprey homolog of the GPi/GPe (also referred to as the dorsal pallidum). (B and C) Retrogradely labeled cells in the GPh (B) following neurobiotin injection (green) into the right dorsal habenula (lateral habenula, Hb) (C). (D and E) Retrogradely labeled striatal (Str) cells (D) following neurobiotin injection (green) into the putative pallidal region (E). (F) Whole-cell recording of a spontaneously firing neuron in the GPh, retrogradely labeled from the habenula. (G) Loose-patch recording of a spontaneous repetitively firing neuron, retrogradely labeled from the habenula, before (mean frequency, 1.3 Hz) and after (mean frequency, 1.35 Hz) the application of the glutamatergic antagonists CNQX (40  $\mu\text{M}$ ) and AP5 (50  $\mu\text{M}$ ). (H) Box plots showing the range and average instantaneous frequency of pallidal neurons before and after application of glutamatergic receptor antagonists ( $n = 6$ ; control; mean,  $1.07 \pm 0.36$ ; CNQX and AP5; mean,  $1.03 \pm 0.31$  Hz). (I) GABA-immunoreactive cells at the level of the GPh. (J–M) Combined retrograde labeling and immunohistochemical detection of GABA, revealing that GABAergic neurons in the GPh are not retrogradely labeled (K–M) from injections (neurobiotin) in the habenula (J). (N) Glutamate immunoreactive cells at the level of the GPh. (O–R) Combined retrograde labeling and immunohistochemical detection of glutamate showing that glutamatergic neurons in the GPh are retrogradely labeled (P–R) from injections (neurobiotin) in the habenula (O). (S and T) Parvalbumin (PV) and calbindin expression in the GPh. Sections are counterstained with a fluorescent Nissl stain. (Scale bars: K and P, 50  $\mu\text{m}$ ; B, D, E, J, O, S, and T, 200  $\mu\text{m}$ ; C, I, N, 500  $\mu\text{m}$ .)



and GPe neurons (Fig. 2D and E and Table S1). Neurons in the GPh exhibited a longer membrane time constant (GPh,  $173.6 \pm 83.2$  ms; GPe/GPi,  $76.4 \pm 38.3$  ms;  $P = 0.001$ ), had a higher input resistance (GPh,  $4.6 \pm 2.2$  G $\Omega$ ; GPe/GPi,  $1.5 \pm 1.2$  G $\Omega$ ;  $P = 0.0003$ ), broader action potential half-widths (GPh,  $7.85 \pm 1.76$  ms; GPe/GPi,  $3.39 \pm 1.36$  ms;  $P = 0.0001$ ), and a higher resting membrane potential (GPh,  $-61.8 \pm 6.2$  mV; GPe/GPi,  $-68.1 \pm 4.4$  mV;  $P = 0.024$ ) than neurons in the GPe/GPi. In addition, a large proportion of GPe/GPi neurons displayed a pronounced voltage-dependent sag in their response to hyperpolarizing current injection (Fig. 2B, *Inset*; GPe/GPi, 4/8; GPh, 1/13) and a larger proportion of GPe/GPi neurons displayed a post-inhibitory rebound depolarization (Fig. 2A and B; GPe/GPi, 5/8; GPh, 5/13).

Together, these results show that neurons in the GPh and GPe/GPi differ in their topographic location, neurotransmitter phenotype (glutamate and GABA), molecular expression, electrophysiological properties, and projections and, therefore, appear to represent distinct classes of pallidal neurons.

**The GPh and GPe/GPi Are Embedded in Independent and Different Circuits.**

The advantageous topographic distinction between habenula and thalamic/brainstem-projecting pallidal neurons in lamprey affords the possibility of untangling the circuitry that influences these separate populations. To address this, a bidirectional tracer, neurobiotin, was injected in the GPh (cases,  $n = 6$ ). In the telencephalon, this resulted in retrogradely labeled neurons in the lateral pallium (LPal), the lower vertebrate equivalent of the cortex, as well as in the striatum (Str) (Fig. 3A and B). Retrogradely labeled cells were also observed in the medial olfactory bulb; however, these cells were also labeled following control injections caudoventral to the GPh (Fig. S1), suggesting that the olfactory cells may have been labeled through fibers of passage. Further caudally in the diencephalon, retrogradely labeled cells were observed in the dorsal thalamus and in two neuromodulatory regions, the periventricular hypothalamus, and the nucleus tuberculi posterior (ntp) (Fig. 3A, D, and F). A subpopulation of neurons in ntp/substantia nigra pars compacta (SNc) (dopaminergic) expressed tyrosine hydroxylase (Fig. 3I),

whereas a subpopulation of the periventricular hypothalamic neurons projecting to the GPh expressed histamine (Fig. 3J). Fibers immunoreactive for tyrosine hydroxylase were observed throughout the GPh (see Fig. 6A).

The inputs to the habenula-projecting GPh and the motor-projecting GPe/GPi, therefore, appear to be distinctly different. Although the input to the GPe/GPi arises from the striatum and the subthalamic nucleus (11), input to the GPh arises directly from the pallium (cortex) and the thalamus in addition to the striatum (Fig. 3A). Furthermore, the GPh does not receive input from the subthalamic nucleus or from GPe-like neurons in the GPe/GPi (Fig. 3C). It, therefore, does not receive input from the so-called indirect pathway that is associated with the motor-related basal ganglia. This suggests that GPh is part of a fundamentally different circuit that is independent from the classical direct and indirect pathways.

The majority of anterogradely labeled fibers passed dorsally from GPh and innervated the homolog of the lateral habenula (Fig. 3B and E and Fig. S1). A second fiber bundle left ventrally and progressed through the hypothalamus and appeared to terminate in the pedunculopontine nucleus (PPN) in the mesencephalon (Fig. 3H), confirming previous studies showing that a few GPh neurons project to the PPN (20). No fibers were observed innervating the brainstem motor regions, including the optic tectum, torus semicircularis and mesencephalic locomotor region (Fig. 3G and H). This confirms previous studies showing that the GPh does not project to the tectum or MLR (18, 19). The major projections of the GPh neurons are, therefore, to the homolog of the lateral habenula. These results indicate that, as with the input, the output circuitry of the GPh is completely distinct from the GPe/GPi, which projects to the thalamus and brainstem motor regions (11, 18–20).

**A Calbindin-Negative Population of Striatal Neurons, Homologous to Striosomes, Projects to GPh.**

The above results suggest that the GPh and GPe/GPi are embedded in separate distinct circuits, with the only potential overlap being that they both receive input from the striatum. In mammals, striatal neurons are located in two distinct compartments, called striosomes that target SNc/ventral

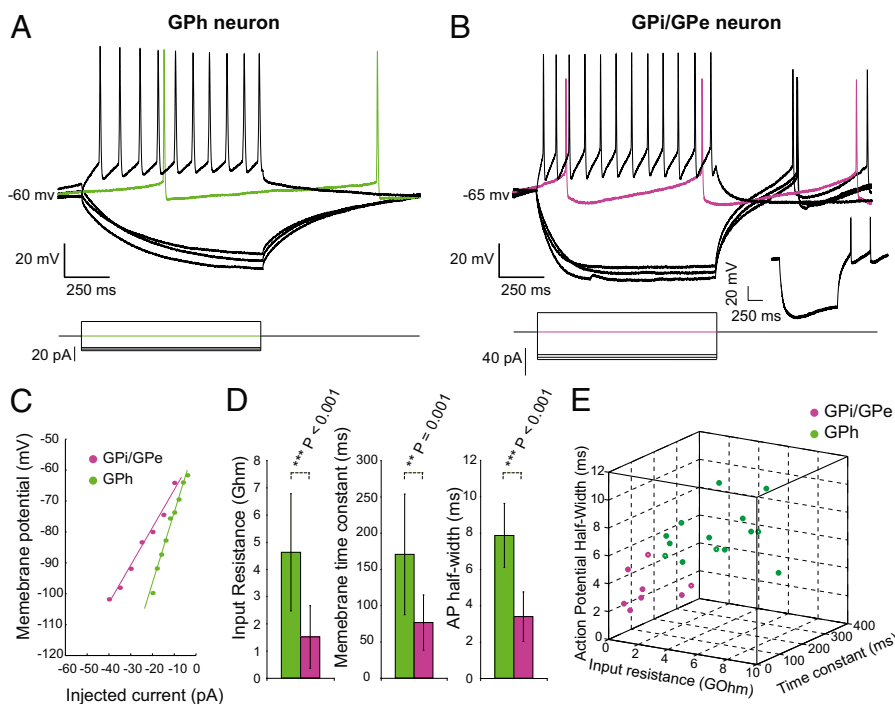


**Fig. 2.** The intrinsic properties of GPh and GPe/GPi neurons differ. (A) Response of a spontaneously active GPh neuron to increasing step current injections. Green trace indicates spontaneous activity without injected current. (B) Response of a spontaneously active GPe/GPi neuron to increasing step current injections. Magenta trace indicates spontaneous activity without injected current. (*Inset*) The voltage-dependent sag induced by a hyperpolarizing current injection. (C) Example of the current-voltage relationship obtained from the GPh (green circles) and the GPe/GPi neuron (magenta circles) represented in A and B. (D) Bar graphs showing the average difference between the input resistance, membrane time constant, and action potential half-width for all of the GPh (green) and GPe/GPi (magenta) neurons. (E) Three-dimensional plot showing the input resistance, membrane time constant, and action potential half-width of each GPh (green dots) and GPe/GPi (magenta dots) neurons. Spontaneously active neurons are represented with filled circles; hollow circles indicate neurons that were not spontaneously active. This clearly indicates that the two types of neurons represent different subpopulations.

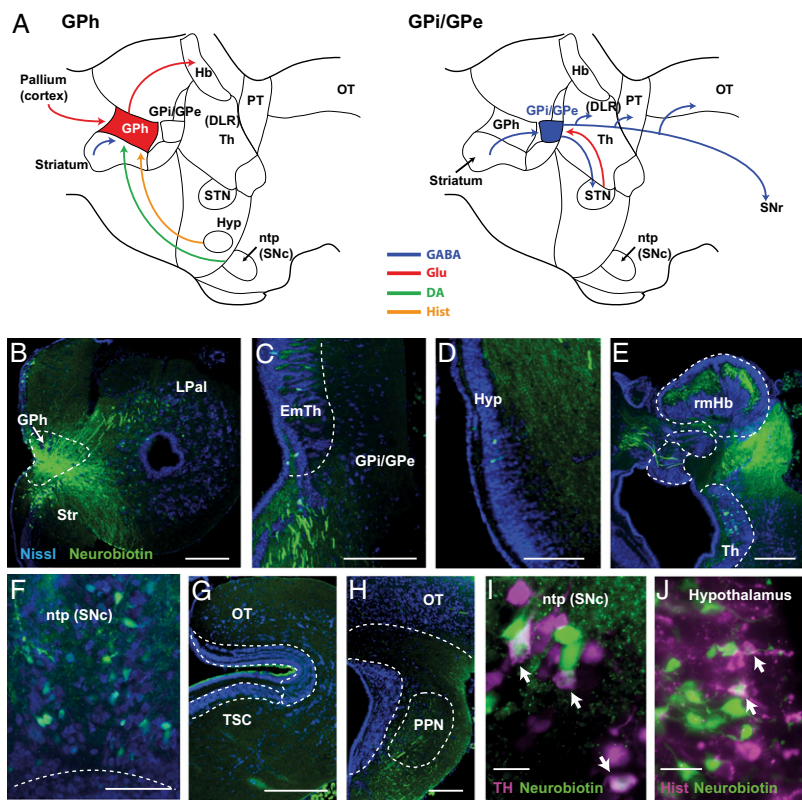


**Fig. 3.** The GPh and GPI/GPe are influenced by independent circuits. (A) Schematic sagittal sections through the lamprey brain showing the connectivity of the GPh and the GPI/GPe. (B) Injection site in the striatum resulting in retrogradely labeled neurons in the striatum (Str) and the lateral pallium (LPal) (B), no labeling in the GPI/GPe (C), retrogradely labeled neurons in the periventricular hypothalamus (Hyp) (D), anterograde labeling in the right dorsal habenula [lateral habenula (Hb)] and retrogradely labeled neurons in the thalamus (Th) (E) and in the ntp (F), and labeled fibers in the PPN (H). No labeling was observed in the brainstem motor regions including the optic tectum (OT), torus semicircularis (TSC), and mesencephalic locomotor region (G and H). All sections are counterstained with a fluorescent Nissl stain (blue). (I) Merged image of the ntp showing retrograde labeling from the GPh (green) and cells immunoreactive for tyrosine hydroxylase (TH) (magenta). (J) Merged image of the hypothalamus showing retrograde labeling from the GPh (green) and cells immunoreactive for histamine (hist, magenta). DLR, diencephalic locomotor region; EmTh, eminentia thalami; PT, pretectum; STN, subthalamic nucleus; Th, thalamus. (Scale bars: B–H, 200  $\mu$ m; I and J, 25  $\mu$ m.)

tegmental area (VTA) and the matriosomes that preferentially express calbindin along with a range of other neurotransmitter-related substances (21–23). To determine whether these striatal subpopulations exist in lamprey and whether they project differentially to the GPh and GPI/GPe, we examined the expression of calbindin, a calcium-binding protein selectively expressed in the striatal matrix (21). Immunohistochemistry revealed that, as with other vertebrates, only a subpopulation of lamprey striatal neurons expressed calbindin (Fig. 4A; cases,  $n = 4$ ). However, neurons retrogradely labeled from the GPh were devoid of calbindin expression (Fig. 4A–D; cases,  $n = 5$ ) and a paucity of calbindin positive fibers were observed in the GPh (Fig. 17), suggesting that the striatal-GPh projection may arise from neurons homologous to striosomes. Consistent with the notion that these calbindin negative neurons might correspond to the striatal striosomes (24), the striatal neurons retrogradely labeled from the homolog of the SNc/VTA were also devoid of calbindin expression (Fig. S2 A–D; cases,  $n = 3$ ). In contrast, a large proportion of the striatal neurons retrogradely labeled from the GPI/GPe expressed calbindin, as with mammalian striatal matrix neurons (Fig. 4 E–H; cases,  $n = 3$ ), and calbindin-positive fibers could be observed in the GPI/GPe and SNr (Fig. S2 E and F; cases,  $n = 2$ ). Together, these results suggest that the GPh and GPI/GPe receive input from separate striatal subpopulations that correspond to the mammalian striosomes and matriosomes, respectively.

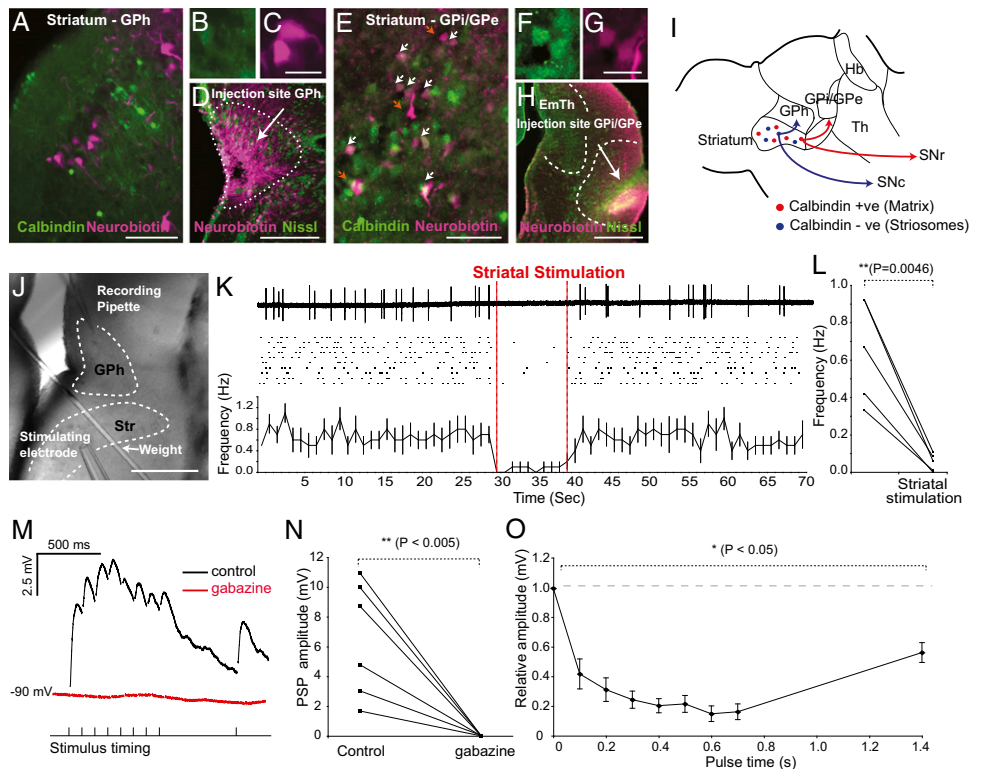
**Striosomes Inhibit GPh Neurons.** To determine how the striatal input influences the firing of GPh neurons, we made recordings in a transverse section that maintains the striato-pallidal projections (Fig. 4J). Extracellular stimulation (1–2 Hz) of the striatum resulted in a significant reduction in the spontaneous firing frequency of all GPh neurons that responded to the stimulation ( $n = 5/8$ ; control,  $0.65 \pm 0.12$  Hz; stimulation,  $0.05 \pm 0.02$  Hz;  $P = 0.0046$ ), completely inhibiting the spontaneous firing in two neurons and reducing the firing rate by over 85% in

the remaining three neurons (Fig. 4 K and L). Whole-cell recordings revealed that stimulation of the striatum evoked depressing synaptic responses [reversed inhibitory postsynaptic potentials (IPSPs)] that were completely abolished by the application of the GABA<sub>A</sub> receptor antagonist gabazine (10  $\mu$ M;  $n = 6$ ; Fig. 4 M–O; paired-pulse depression,  $0.41 \pm 0.8$ ). This was quantified by comparing the amplitude of the first postsynaptic potential (PSP) before and after drug application (control PSP1,  $5.19 \pm 2.35$  mV; gabazine PSP1,  $0.027 \pm 0.03$  mV;  $P < 0.001$ ;  $n = 6$ ).

Together, these results show that a subpopulation of striatal neurons, equivalent to the striosomes, project to and inhibit the spontaneously active GPh neurons. These results suggest that the GPh and GPI/GPe neurons receive input from striosomes and matriosomes, respectively (Fig. 4I). The striosomes may, therefore, be the source of reward-related information that inhibits the habenula-projecting pallidal neurons in response to reward or reward prediction (5, 14).

**Direct Glutamatergic Projections from the Pallium (Cortex) Excite Neurons in the GPh.** Our next aim was to determine whether the direct projection from the lateral pallium (cortex) to the GPh would provide excitation and increase their firing. Dual-tracer injections and confocal microscopy first confirmed that pallial fibers could be observed throughout the GPh, where they formed direct putative contacts with the projection neurons (Fig. 5 A–D and F; cases,  $n = 6$ ). To determine how the pallial input influenced the firing of GPh neurons, we made recordings in a transverse section that maintained the pallio-GPh projections (Fig. 5E). Extracellular stimulation (1–10 Hz) of the pallium resulted in a significant increase in the spontaneous firing frequency of all GPh neurons that responded to the stimulation ( $n = 9/12$ ; control,  $0.74 \pm 0.16$  Hz; stimulation,  $2.79 \pm 0.51$  Hz;  $P = 0.003$ ) (Fig. 5 G and H). Whole-cell recordings revealed that stimulation of the pallium evoked excitatory synaptic potentials (Fig. 5I;  $n = 14$ ). Both the synaptic potentials and the increase in

**Fig. 4.** Striatal neurons, homologous to striatal striosome neurons, inhibit the spontaneous activity of GPh neurons. (A–C) Neurobiotin retrogradely labeled neurons, following an injection in the GPh (magenta) (D) and calbindin immunoreactive neurons (green) in the striatum (Str). (E–G) Neurobiotin retrogradely labeled neurons, following an injection in the GPI/GPe (magenta) (H) and calbindin-immunoreactive neurons (green) in the striatum. (I) Schematic representation of the projections from the calbindin positive and negative striatal subpopulations. (J) Photomicrograph showing the location of the stimulating and recording electrodes in a transverse section of the lamprey brain. (K) Loose-patch recording and raster plot of a spontaneously active neuron in the GPh showing the effect of striatal stimulation. (L) Graph showing the spontaneous firing frequency before and during striatal stimulation. (M) IPSPs (reversed IPSPs) recorded in a spontaneously active GPh neuron following striatal stimulation before and after the application of gabazine (10  $\mu$ M), a GABA<sub>A</sub> receptor antagonist. (N) Graph showing the amplitude of the first PSP before and after the application of gabazine. (O) Average postsynaptic responses of all neurons normalized to the amplitude of the first PSP. All stimulation artifacts were manually removed. Hb, habenula; Th, thalamus. (Scale bars: A and E, 100  $\mu$ m; D, H, and J, 200  $\mu$ m; C and G, 25  $\mu$ m.)



firing frequency could be completely abolished by the application of glutamate receptor antagonists CNQX (40  $\mu$ M) and AP-5 (50  $\mu$ M) [Fig. 5 I and J;  $n = 6$  (control,  $0.57 \pm 0.15$  Hz; stimulation,  $0.47 \pm 0.05$  Hz;  $P = 0.26$ );  $n = 5$  (control PSP1,  $7.18 \pm 4.53$  mV; CNQX plus AP5 PSP1,  $0.039 \pm 0.028$  mV;  $P = 0.011$ )]. Together, our results indicate that there are direct excitatory (glutamatergic) inputs from the pallium (cortex) to the GPh. The direct pallio-GPh projection may, therefore, be the source of reward-related information that can increase the firing rate of habenula-projecting pallidal neurons in response to errors in reward prediction or when an adverse outcome is expected (14).

**Individual GPh Neurons Integrate Excitatory Input from the Pallium (Cortex) with Inhibitory Input from Striosomes.** To determine whether single GPh neurons integrated this excitatory input with the inhibitory input from the striatum, we stimulated the striatum in the presence of glutamatergic antagonists (40  $\mu$ M CNQX and 50  $\mu$ M AP5) while recording from neurons that responded to pallial stimulation. Striatal stimulation resulted in a reduction in the firing rate of all GPh neurons that responded to striatal stimulation (Fig. 5G;  $n = 3/5$ ; control,  $0.45 \pm 0.25$  Hz; stimulation,  $0.04 \pm 0.06$  Hz;  $P = 0.02$ ). These results indicate that neurons in the GPh integrate excitatory input from the pallium with monosynaptic inhibitory input from the striatum.

To determine whether our stimulation recruited both direct excitatory projections, as well as oligosynaptic inhibitory projections, we applied the GABA<sub>A</sub> receptor antagonist (gabazine) after stimulating the pallium. Application of the antagonist resulted in an increase in the synaptic responses in all neurons recorded, typically after the second pulse (Fig. 5K;  $n = 6$ ), as quantified by comparing the normalized area under the response ( $116 \pm 7\%$  compared with control;  $P = 0.002$ ; Fig. 5L). Furthermore, application of gabazine changed the synaptic dynamics from paired-pulse depression to facilitation (PPF) ( $1.59 \pm 0.4$ ;

Fig. S3). These results indicate that our pallial stimulation recruits direct excitatory projections, as well as oligosynaptic inhibition, likely via pallio-striatal-GPh projections. The pallium can, therefore, influence the GPh in two ways: either through direct pallial-GPh projections or through an indirect pallial-striatal-GPh projection.

To determine whether there are separate pallial populations that can drive these circuits, we made dual-tracer injections in the striatum and GPh. This revealed that there was little overlap in the pallial populations projecting to striatum and GPh (Fig. 5M–P; cases,  $n = 4$ ). In addition, a 2D density analysis revealed that these pallial populations were also spatially segregated (Fig. 5M and Fig. S4). The pallio-GPh neurons were located preferentially in the dorsal lateral pallium, whereas the pallio-striatal neurons were preferentially located in the ventral lateral pallium. This suggests that the pallio-striatal and pallio-GPh projections may arise from separate pallial (cortical) subpopulations.

**Dopamine Reduces the Spontaneous Firing Frequency of Dopamine D2 Receptor-Expressing GPh Neurons.** To determine how the dopaminergic innervation of the GPh affects neuronal firing, we first examined the dopamine receptor expression. In lamprey, dopamine D2 receptors are highly expressed in the striatum as well as in the GPh (25). In situ hybridization confirmed that neurons in the GPh express D2 receptor mRNA (Fig. 6B; cases,  $n = 5$ ). In contrast, no D2 receptor expression was observed further caudally in the GPI/GPe (Fig. 6D). In addition, very few tyrosine hydroxylase immunoreactive fibers were observed in the GPI/GPe (Fig. 6C) but are observed in the GPh (Fig. 6A), and retrograde tracing from the GPI/GPe has not revealed a projection from the ntp to the GPI/GPe (11). To confirm that the D2 receptor expressing neurons in the GPh project to the habenula, we combined retrograde labeling with in situ hybridization. This revealed that a subpopulation of retrogradely labeled GPh

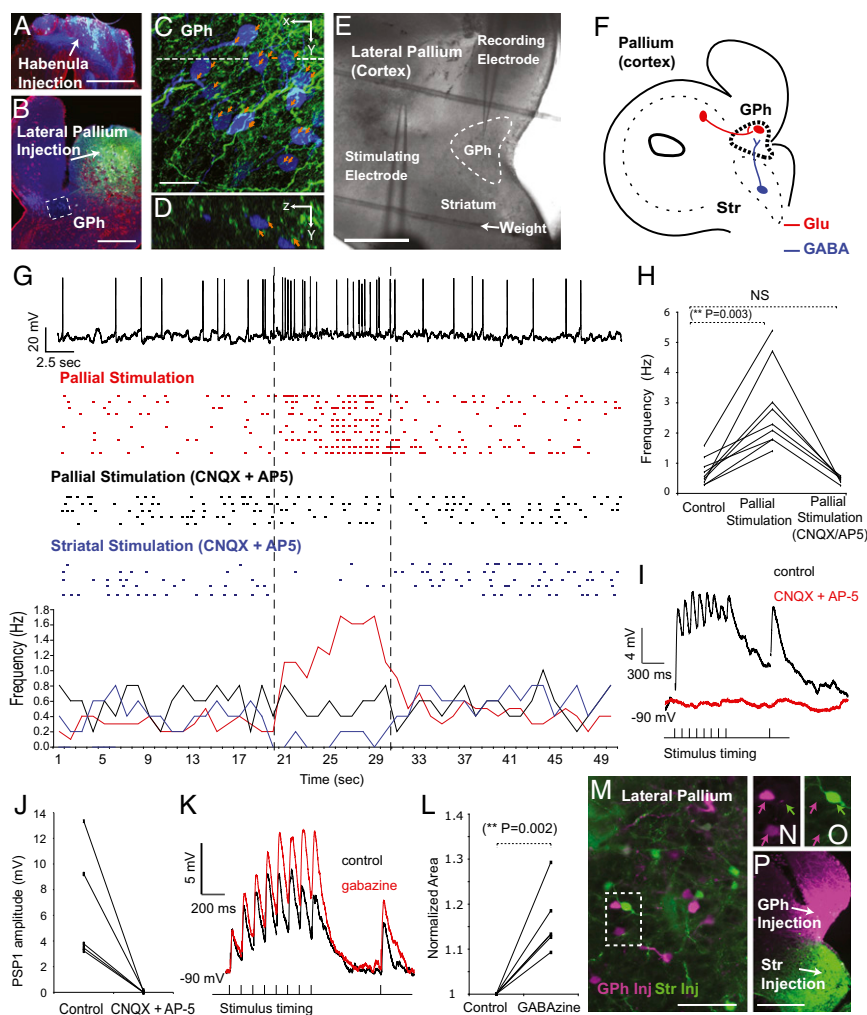


**Fig. 5.** Direct glutamatergic (Glu) projections from the pallium (cortex) excite neurons in the GPh. (A–D) Confocal photomicrograph showing that anterogradely labeled fibers (green) (C and D) from the pallium (B) form direct putative contacts (red arrows) with retrogradely labeled GPh neurons (blue) (A, C, and D). (E) Photomicrograph showing the location of the stimulating and recording electrodes in a transverse section of the lamprey brain. (F) Schematic representation of the projections from the pallium and striatum to the GPh. (G) Whole-cell recording and raster plot of a spontaneously active neuron in the GPh showing the effect of pallial and striatal stimulations. (H) Graph showing the spontaneous firing frequency before, during pallial stimulation and following application of the glutamatergic antagonists CNQX 40  $\mu$ M and AP5 50  $\mu$ M. (I) PSPs recorded in a spontaneously active GPh neuron following pallial stimulation, before and after (red trace) the application of CNQX (40  $\mu$ M) and AP-5 (50  $\mu$ M), which abolishes the EPSPs. (J) Graph showing the amplitude of the first PSP before and after the application of CNQX and AP-5. (K) PSP recorded in a spontaneously active GPh neuron following pallial stimulation, before and after the application of the GABA<sub>A</sub> receptor antagonist gabazine 10  $\mu$ M. (L) Graph showing the normalized area under the graph before and after the application of gabazine. (M–P) Retrogradely labeled neurons in the pallium following injection in the GPh (magenta) and striatum (Str) (green) (P). All stimulation artifacts were manually removed. (Scale bars: C, 25  $\mu$ m; M, 100  $\mu$ m; A, B, E, and P, 200  $\mu$ m.)

neurons expressed D2 receptor mRNA (Fig. 6 E–H; cases,  $n = 3$ ).

In lamprey, as with other vertebrates, dopamine can cause a reduction in the excitability of neurons through activation of the D2 receptor (25). This suggested that activation of the GPh D2 receptors might lead to a decrease in the activity of the spontaneously active neurons. Indeed, bath application of the selective D2 receptor agonist TNPA [R(-)-2,10,11-trihydroxy-N-propyl-noraporphine 123 hydrobromide hydrate] (100  $\mu$ M) resulted in a significant reduction in the spontaneous firing frequency in 7 of 11 GPh neurons (control,  $0.9 \pm 0.2$  Hz; TNPA,  $0.53 \pm 0.13$  Hz;  $P = 0.031$ ;  $n = 11$ ; Fig. 6 I–K). In one case, a modest increase in firing frequency occurred following TNPA application (0.5–0.85 Hz); in all other cases, the application of TNPA had no effect on the firing frequency, even after 20 min of drug application. In mammals and lamprey, the habenula-projecting pallidal neurons drive activity in the lateral habenula, which exerts an indirect inhibitory influence on dopamine neurons (12, 26, 27). Our results, therefore, show that dopamine projections back to the GPh close this loop and could form a positive-feedback circuit to regulate the dopaminergic system (Fig. 6L).

## Discussion

Together, our results show that in addition to the direct and indirect pathways an, additional circuit exists within the basal ganglia that control the GPh. Because the GPh neurons, the

output of this circuit, are known to respond to the predicted and actual value of actions, we suggest that the circuit we identify here may predict and evaluate the outcome of actions that are selected by the classic direct and indirect pathways (Fig. S5).

### Pallial (Cortical) Projections to the GPh Could Provide Excitation in Response to Errors in Prediction.

The habenula-projecting pallidal neurons have previously been shown to be excited when an adverse outcome is predicted or when an outcome is worse than expected (reward-prediction error) and are inhibited by the reverse conditions (13, 14). Our results in lamprey demonstrate that direct excitatory projections from the pallium, the lower vertebrate equivalent of the cortex, can increase the firing rate of GPh neurons and may represent the source of excitation that increases GPh activity in response to errors in reward prediction.

In mammals, direct cortico-pallidal projections have rarely been reported; nonetheless, a few studies have indicated that they may exist (28–30), as first suggested based on axon degeneration studies (28, 29). More recently, a combined anterograde-labeling and electron microscopy study has confirmed that areas of the frontal cortex in rat, including the insular, orbitofrontal, and anterior cingulate cortex, project to the entopeduncular nucleus (30). Whether these projections selectively target the habenula-projecting entopeduncular (EPH) neurons remains to be determined. Interestingly, neurons in these cortical areas encode reward-related information (31, 32), and microstimulation of the cingulate cortex in primates is aver-

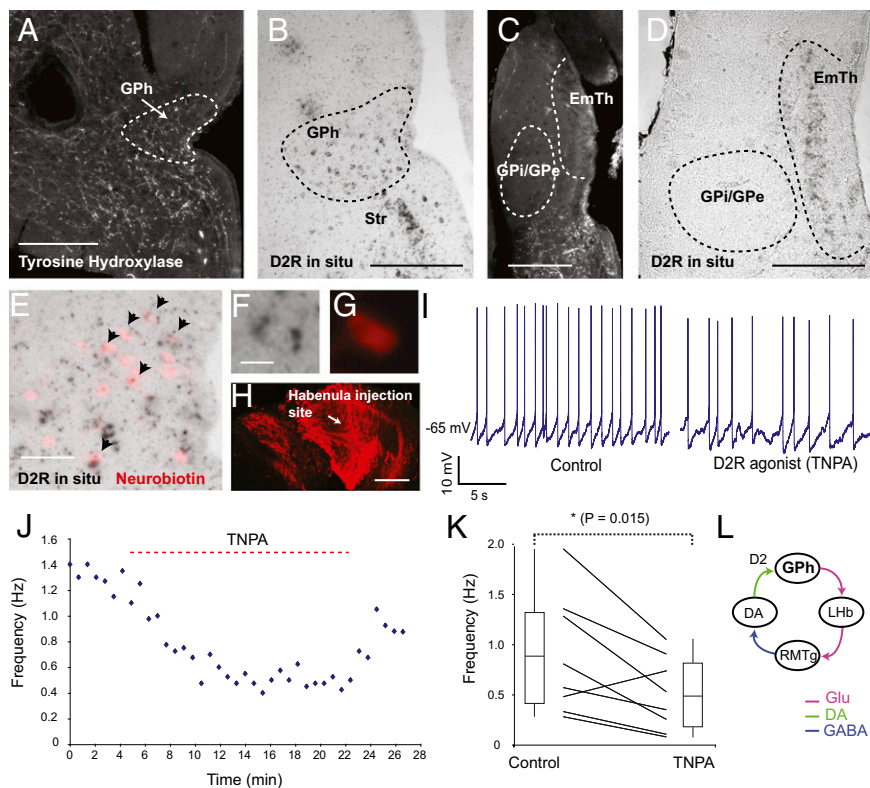


**Fig. 6.** Dopamine reduces the spontaneous firing frequency of dopamine D2 receptor (D2R) expressing GPh neurons. (A) Tyrosine hydroxylase immunoreactivity in the striatum (Str) and GPh. (B) Neurons in the GPh express D2R mRNA. (C) Lack of tyrosine hydroxylase immunoreactivity in the GPi/GPe. (D) D2R mRNA expression at the level of the GPi/GPe. (E–H) Neurobiotin retrogradely labeled neurons (pink) in the GPh following an injection in the habenula (red) (E, G, and H) and neurons expressing D2R mRNA (black) (F). (I) Whole-cell recording of spontaneous GPh activity before and after the application of the dopamine D2 receptor agonist TNPA (100  $\mu$ M). (J) Firing frequency–time plot showing how the firing frequency of a GPh neuron changes with the application of TNPA. (K) Graph showing the average firing frequency of GPh neurons before and after the application of TNPA. (L) Schematic drawing of the feedback loop between the GPh and dopaminergic (DA) neurons. EmTh, eminentia thalami; LHb, lateral habenula. (Scale bars: A–D and H, 200  $\mu$ m; E, 100  $\mu$ m; F and G, 20  $\mu$ m.)

sive and can increase the negative valence of a possible choice (33). Together, this further supports our suggestion that direct pallio/cortico-pallidal projections provide the excitatory drive to the GPh neurons in response errors in reward prediction or in expectation of an adverse outcome.

Classically, neurons in the entopeduncular (EP)/GPi receive excitatory input from the subthalamic nucleus (34). However, in vivo electrophysiological recordings in rodents and cats have revealed that EP neurons are actually inhibited by stimulation of the subthalamic nucleus (35, 36), whereas the majority of EP neurons projecting to the thalamus are indeed excited by this stimulation (35, 37, 38). These results suggest that as in lamprey, EP neurons do not receive a direct excitatory input from the subthalamic nucleus but, rather, are inhibited through some unknown pathway. Together with our results, this suggests that direct cortico-pallidal projections may be conserved in mammals and provide the excitatory input to the habenula-projecting pallidum.

**Striosomal Inhibition of GPh Decreases the Activity in Response to the Prediction of Reward.** In primates, GPh neurons are inhibited when reward is predicted or when an outcome is better than expected (13, 14). Our results demonstrate that striatal neurons located in striosomes can provide the source of input that could inhibit GPh neurons in response to reward prediction. This inhibitory pathway from the striosomes to the GPh/EPH may also be present in mammals, because striosome neurons have been reported to innervate the rostral entopeduncular nucleus, where the EPH neurons are primarily located (10). The striosomes in mammals have also been implicated in reward-related behavior (39, 40), further suggesting that the striosomes-EPH projection may be responsible for inhibiting the EPH neurons in response to prediction of reward.

Our results show that pallio/cortico-GPh and striosome-GPh projections have a dichotomous effect on GPh neuronal firing and that single GPh neurons integrate inputs from these two

sources. GPh neurons may, therefore, integrate both positive- and negative-reward signals from the striosomes and pallium/cortex, respectively (Fig. 7). In mammals, the EPH exerts an excitatory influence on the lateral habenula (16), which, in turn, indirectly, via the rostromedial tegmental nucleus (RMTg), inhibits dopaminergic neurons in the VTA and SNc (15, 17, 27, 41, 42). The organization of the lateral habenula and its downstream targets is exceptionally well conserved (12). Consequently, changes in the firing rate of GPh neurons through activation of excitatory pallio-GPh and inhibitory striosome-GPh projections will lead to a decrease or increase in dopaminergic firing, respectively. These pathways may therefore convey opposing motivational signals, pallio-GPh-habenula projections could suppress dopaminergic firing when an outcome is worse than expected. In contrast, the striato-GPh-habenula projections could remove the inhibition of the dopaminergic system if a positive reward is expected or the outcome of an action is better than expected.

**Dopaminergic Modulation of GPh.** Our results also show that the GPh-lateral habenula-RMTg-dopamine projections do not exert a unidirectional influence on the dopaminergic system, rather dopaminergic feedback to the GPh can inhibit the firing of these pallidal neurons. Consequently, the dopaminergic and GPh populations have an opposing influence on each other. This dopaminergic feedback circuit is likely to exist in mammals as a subpopulation of pallidal neurons express dopamine D2 receptors (43) and dopamine release can induce a decrease in pallidal discharge that is dependent on dopamine D2 receptors (44, 45). In addition, the dopaminergic innervation of the primate globus pallidus is conspicuously high in the regions where the GPh neurons are located (46), suggesting that the dopaminergic feedback may selectively target GPh neurons.

**Evolutionary Differences.** While the circuitry regulating the GPh is likely to be conserved throughout the vertebrate phylum, (Fig. 7C) the habenula and thalamic/brainstem projecting pallidal

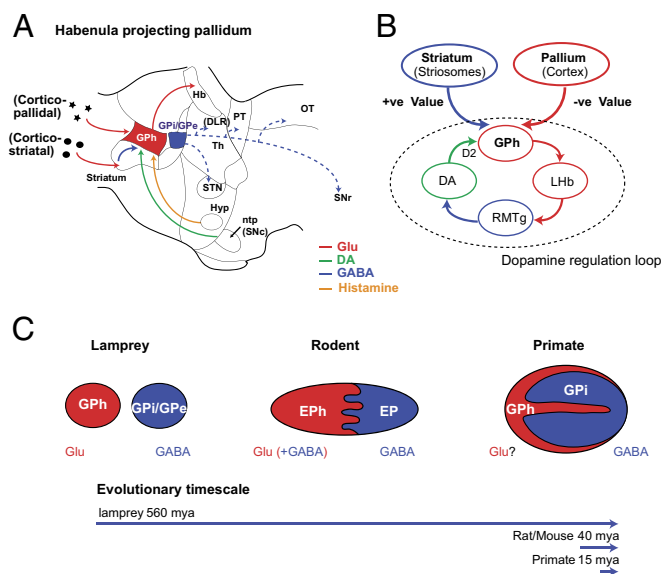


**Fig. 7.** GPh circuit. (A) Schematic drawing showing the connectivity of the GPh and the GPI/GPe together with their neurotransmitter phenotype. (B) Schematic drawing showing the proposed valuation and dopamine-regulation circuit in which the GPh is embedded. (C) Schematic representation of the GPh and GPI/GPe compartments. They are represented in separate nuclei in lamprey; in rodents (10, 16), EP<sub>h</sub> and EP are merged into two compartments within one nucleus; and in primates (9), the habenular projecting part is mostly at the periphery, also referred to as the border region of the globus pallidus (26). Below the evolutionary timescale is indicated. DA, dopamine; DLR, diencephalic locomotor region; EP, entopeduncular nucleus; Glu, glutamate; Hyp, hypothalamus; LHb, lateral habenula; OT, optic tectum; PT, pretegmentum; STN, subthalamic nucleus; Th, thalamus.

neurons in rodents (10) and primates (9) are not located in a separate nucleus, as they are in lamprey. Nonetheless, these populations are located in a topographically separate location, in the rostral EP or border region of the globus pallidus, a region also referred to as the border region of the globus pallidus (GP<sub>b</sub>) (26). Furthermore, the difference in neurotransmitter may also be conserved, because the majority of GPh neurons in rodents have recently been shown to be glutamatergic and are able to directly excite neurons in the lateral habenula (16). However, in contrast to our results, a significant proportion of these GPh neurons are GABAergic (16, 47). Consequently, it appears that during evolution a second (GABAergic) population of GPh neurons evolved.

## Conclusion

Together, our results show that in addition to the direct and indirect pathways, which control action selection, an additional evaluation circuit exists within the basal ganglia that regulates the GPh and the downstream dopamine neurons (12). Because this circuit is present in lamprey, one of the phylogenetically oldest vertebrates, it suggests that separate circuits for selecting and evaluating the outcome of actions evolved at the dawn of vertebrate evolution. Consequently, the basal ganglia and associated habenula circuitry may comprise the core elements that all vertebrates use to select appropriate actions and evaluate their outcome.

## Experimental Procedures

Experiments were performed on a total of 53 adult river lampreys (*Lampetra fluviatilis*). The experimental procedures were approved by the local ethics committee (Stockholms Norra Djurförsöksetiska Nämnd) and were in accordance with *The Guide for the Care and Use of Laboratory Animals* (48).

During the investigation, every effort was made to minimize animal suffering and to reduce the number of animals used.

**Tracing.** The animals were deeply anesthetized in 100 mg/L Tricaine methane sulfonate (MS-222) (Sigma) diluted in fresh water. They were then transected caudally at the seventh gill, and the dorsal skin and cartilage were removed to expose the brain. During the dissection and the injections, the head was pinned down and submerged in ice-cooled oxygenated Hepes-buffered physiological solution (138 mM NaCl, 2.1 mM KCl, 1.8 mM CaCl<sub>2</sub>, 1.2 mM MgCl<sub>2</sub>, 4 mM glucose, and 2 mM Hepes), pH 7.4.

All injections for retrograde and anterograde tracing were made with glass (borosilicate, OD = 1.5 mm, ID = 1.17 mm) micropipettes, with a tip diameter of 10–20 μm. The micropipettes were fixed in a holder, which was attached to an air supply and a Narishige micromanipulator. Neurobiotin [50–200 nL; Vector; 20% (wt/vol) in distilled water containing Fast Green to aid visualization of the injected tracer] or Alexa Fluor 488-dextran [10 kDa; 12% (wt/vol) in distilled water; Molecular Probes Europe] was pressure injected unilaterally into (i) habenula-projecting dorsal pallidum, (ii) dorsal pallidum, (iii) habenula, (iv) lateral pallidum, and (v) striatum.

Following injections, the heads were kept submerged in Hepes in the dark at 4 °C for 24 h to allow retrograde transport of the tracers. The brains were then dissected out of the surrounding tissue and fixed by immersion in 4% formalin and 14% saturated picric acid in 0.1 M phosphate buffer (PB) (pH 7.4) for 12–24 h, after which, they were cryoprotected in 20% (wt/vol) sucrose in PB for 3–12 h; 20-μm-thick transverse sections were made using a cryostat, collected on gelatin-coated slides, and stored at –20 °C until further processing. For GABA and glutamate immunohistochemistry, animals were perfused through the ascending aorta with 4% formalin, 2% (GABA), or 0.5% (glutamate) glutaraldehyde, and 14% of a saturated solution of picric acid in PB. The brain was postfixed for 24–48 h and cryoprotected as described above.

**Immunohistochemistry.** For immunohistochemical detection of tyrosine hydroxylase, histamine, glutamate, and GABA in the projection neurons, the GPh or habenula was injected and brains were processed as described above. All primary and secondary antibodies were diluted in 1% BSA and 0.3% Triton-X 100 in 0.1 M PB. Sections were incubated overnight with rabbit anti-histamine antibody [1:10,000, 19C; kindly donated by Pertti Panula (University of Helsinki, Helsinki)], mouse monoclonal anti-tyrosine hydroxylase antibody (1:200; MAB318; Millipore), rabbit anti-glutamate antibody (1:500; AB133; Millipore), or mouse monoclonal anti-GABA antibody [1:5,000, mAb 3A12, kindly donated by Peter Streit (Brain Research Institute, University of Zürich, Zürich)]. Sections were subsequently incubated with a mixture of Neurotrace deep-red (1:500; Molecular Probes), Cy2-conjugated streptavidin (1:1,000; Jackson ImmunoResearch) and Cy3-conjugated donkey anti-rabbit IgG, or Cy3-conjugated donkey anti-mouse IgG (1:500; Jackson ImmunoResearch) for 2 h and coverslipped in glycerol containing 2.5% diazabicyclooctane (DABCO) (Sigma).

For the immunohistochemical detection of parvalbumin and calbindin, brains were dissected out and processed as described above. Sections were then incubated overnight with either a rabbit polyclonal anti-parvalbumin antibody (1:1,000; Swant; PV-28, 5.5 raised against parvalbumin isolated from rat muscle), mouse monoclonal anti-calbindin-D28K antibody (1:2,000; C9848; Sigma-Aldrich). Sections were subsequently incubated with Cy3-conjugated donkey anti-rabbit IgG or donkey anti-mouse IgG (1:500; Jackson ImmunoResearch) for 2 h and coverslipped.

**Analysis.** Photomicrographs of key results were taken with an Olympus XM10 digital camera mounted on an Olympus BX51 fluorescence microscope (Olympus Sverige). Illustrations were prepared in Adobe Illustrator and Adobe Photoshop CS4. Images were only adjusted for brightness and contrast. Confocal Z-stacks of the sections were obtained using a Zeiss Laser scanning microscope 510, and the projection images were processed using the Zeiss LSM software and Adobe Photoshop CS4.

For the density analysis, the locations of neurons were plotted with respect to the ventral and lateral border of the lateral pallidum using Olympus Cell<sup>A</sup> software (Version 3.1). One-dimensional kernel density estimates were obtained using the R (R Foundation for Statistical Computing; [www.r-project.org](http://www.r-project.org)) “density” function. The 2D kernel density estimations used to compute the distribution contours were obtained using the “kde2d” function provided in the Modern Applied Statistics with S (MASS)-library (49), and bandwidths in the density estimation were chosen using the “bandwidth.nrd” function. Two-dimensional kernel density estimation were graphically displayed as contour plots, with the contour lines connecting

points of equal densities and drawn for density values between 20% and 100% of the estimated density range, in steps of 10%.

**In Situ Hybridization.** Templates for in vitro transcription were prepared by PCR amplification. For the dopamine D2 receptor probe, a 660-bp fragment was obtained using 5'-TGCTCATATGCCTCATCGTC-3' forward and 5'-TCAAGCTTTGCACAATCGTC-3' reverse primers (25). The amplified cDNA fragments were cloned into a pCRII-TOPO vector (Invitrogen), cleaned, and confirmed by nucleotide sequencing (KIGene core facility at Karolinska Institutet). Linearized plasmids (1  $\mu$ g) were used to synthesize digoxigenin (DIG)-labeled riboprobes. In vitro transcription was carried out using the DIG RNA Labeling Mix (Roche Diagnostics) according to the manufacturer's instructions. The transcripts were purified using NucAway spin columns (Applied Biosystems). Sense probes were used as negative controls.

The habenular neurobiotin-injected animals were deeply anesthetized in MS-222 diluted in fresh water and killed by decapitation. Brains were quickly removed and fixed in 4% paraformaldehyde in 0.01M PBS overnight at 4 °C. They were afterward cryoprotected in 30% sucrose in 0.01 M PBS overnight, and 20- $\mu$ m-thick serial, transverse cryostat sections were obtained and immediately used for in situ hybridization. The sections were left at room temperature for 30 min, washed in 0.01 M PBS, acetylated in 0.25% acetic anhydride in 0.1 M triethanolamine (pH 8.0) for 5 min, washed in 0.01 M PBS, and prehybridized [50% formamide, 5 $\times$  SSC (pH 7.0), 5 $\times$  Denhardt's solution, 500  $\mu$ g/mL salmon sperm DNA, 250  $\mu$ g/mL yeast RNA] for 2–4 h at 60 °C. DIG-labeled D2 receptor riboprobes were prepared and added to the hybridization solution to a final concentration of 500 ng/mL, and parallel series were hybridized overnight at 60 °C. An RNase treatment (20  $\mu$ g/mL in 2 $\times$  SSC) was performed for 30 min at 37 °C following stringent washes in SSC (Applied Biosystems). After additional washes in maleic acid buffer (MABT) (pH 7.5), the sections were incubated overnight at 4 °C in anti-digoxigenin Fragment antigen-binding fragments conjugated with alkaline phosphatase (1:2,000; Roche Diagnostics) in 10% heat inactivated normal goat serum (Vector Laboratories). Several washes in MABT were carried out, and the alkaline phosphatase reaction was visualized using nitro blue tetrazolium chloride/5-bromo-4-chloro-3-indolyl-phosphate (NBT/BCIP) substrate (Roche Diagnostics) in staining buffer [0.1 M Tris buffer (pH 9.5) containing 100 mM NaCl and 5 mM levamisole]. The staining process was stopped with washes in PBS. Those sections that had been subjected to retrograde tracing with neurobiotin were subsequently incubated with streptavidin conjugated to Cy3 (1:1,000; Molecular Probes). Sections were coverslipped with glycerol containing 2.5% DABCO (Sigma-Aldrich).

**Electrophysiology.** Tracing before slice preparation for electrophysiology. When tracer injections were combined with electrophysiological recordings, the brain was accessed by opening the skull from the level of the olfactory bulb and caudally until the obex. Throughout this procedure, the bath was perfused with Hepes solution containing MS-222 (1 mg/100 mL). The fluorescent tracer tetramethylrhodamine coupled to 3-kDa dextran (12% in distilled water; Molecular Probes) was injected as described above into the habenula. Following the procedure, animals survived for 12–18 h before physiological slices of the brain were prepared.

The dissection and removal of brains from deeply anesthetized (MS-222; 100 mg l<sup>-1</sup>; Sigma) animals were performed as described above. To facilitate the cutting of slices on a microtome (Microm HM 650V; Thermo Scientific), brains were embedded in liquid agar (Sigma; 4% dissolved in water). The

agar block containing the brain was then glued to a metal plate and transferred to ice-cold artificial cerebrospinal fluid (aCSF) with the following composition (in mM): NaCl, 125; KCl, 2.5; MgCl<sub>2</sub>, 1; NaH<sub>2</sub>PO<sub>4</sub>, 1.25; CaCl<sub>2</sub>, 2; NaHCO<sub>3</sub>, 25; glucose, 8. The aCSF was oxygenated continuously with 95% O<sub>2</sub> and 5% CO<sub>2</sub> (pH 7.4). Transverse brain slices of 350–400  $\mu$ m were cut at the level of the striatum and allowed to recover at ~5 °C for at least 1 h before being transferred to a submerged recording chamber. Perfusion of the slices was performed with aCSF at 6–8 °C (Peltier cooling system; Elfa).

Whole-cell current-clamp recordings were performed with patch pipettes made from borosilicate glass microcapillaries (Hilgenberg) using a horizontal puller (Model P-97; Sutter Instruments). The resistance of recording pipettes were typically 7–12 M $\Omega$  when filled with intracellular solution of the following composition (in mM): potassium gluconate, 131; KCl, 4; phosphocreatine disodium salt, 10; Hepes, 10; Mg-ATP, 4; Na-GTP, 0.3 (osmolarity 265–275 mOsmol). Bridge balance and pipette-capacitance compensation were adjusted for on the MultiClamp 700B and Digidata 1322 (Molecular Devices). Membrane potential values were not corrected for the liquid junction potential (~10 mV).

Extracellular stimulation of usually 100- $\mu$ s duration (range 50–300  $\mu$ s) of pallial and striatal efferents was performed with a glass pipette electrode, connected to a stimulus isolation unit (MI401; University of Cologne, Zoological Institute). The stimulation intensity was set to about one to two times the threshold strength (typically 50–100  $\mu$ A) to evoke PSPs. To investigate the short-term dynamics of synaptic transmission, a stimulus train of eight pulses at 10Hz was used together with a recovery test pulse 600 ms after the eighth pulse (50). PSPs often started on the decay phase of previous responses, and to extract correct amplitudes the synaptic decay was either fitted by an exponential curve and subtracted or manually subtracted (44). The paired-pulse ratio was calculated by dividing the second PSP by the first PSP in a response train.

The neurons were visualized with differential interference contrast/infrared optics (Zeiss Axioskop 2F5 Plus or Olympus BX51WI). Retrogradely labeled cells were illuminated with a mercury lamp (Zeiss HBO 100 or Olympus U-RFL-T) for a brief period to avoid bleaching and visualized in the microscope using a fluorescent filter cube. Labeled neurons were photographed before switching back to DIC/infrared for patching of identified labeled neurons. Glutamate receptor antagonists AP5 (50  $\mu$ M; Tocris) and CNQX (40  $\mu$ M; Tocris), GABAA receptor antagonist gabazine (10  $\mu$ M), and the D2 receptor agonist TNPA (200  $\mu$ M) were all bath-applied. Data collection was made using a MultiClamp 700B and Digidata 1322 (Molecular Devices). Data analyses were made using custom written scripts in Matlab.

**Statistics and Data Presentation.** Statistical analysis of the data were made with Matlab using two-sample *t* test; the significance threshold was  $P < 0.05$ . Box plots were used for graphic presentation, with central line representing the mean; interquartile range is marked by the box and overall distribution by the whiskers. Sample statistics are expressed as means  $\pm$  SEM. In the figures, significance is indicated as follows: \* $P < 0.05$ ; \*\* $P < 0.01$ ; and \*\*\* $P < 0.001$ .

**ACKNOWLEDGMENTS.** We thank Prof. Abdel El Manira for valuable comments on the manuscript. This work was supported by Swedish Research Council Grants Vetenskapsrådet-Medicin 3026 and Vetenskapsrådet-Naturvetenskap och Teknik 621-2007-6049; European Union Seventh Framework Programme Select-and-Act Grant 201716; the European Union Cortex Training Program; and research funds from Karolinska Institutet.

- Hikosaka O, Takikawa Y, Kawagoe R (2000) Role of the basal ganglia in the control of purposive saccadic eye movements. *Physiol Rev* 80(3):953–978.
- Kravitz AV, et al. (2010) Regulation of parkinsonian motor behaviours by optogenetic control of basal ganglia circuitry. *Nature* 466(7306):622–626.
- Redgrave P, Prescott TJ, Gurney K (1999) The basal ganglia: A vertebrate solution to the selection problem? *Neuroscience* 89(4):1009–1023.
- Garrison J, Erdeniz B, Done J (2013) Prediction error in reinforcement learning: A meta-analysis of neuroimaging studies. *Neurosci Biobehav Rev* 37(7):1297–1310.
- Graybiel AM (2008) Habits, rituals, and the evaluative brain. *Annu Rev Neurosci* 31: 359–387.
- O'Doherty J, et al. (2004) Dissociable roles of ventral and dorsal striatum in instrumental conditioning. *Science* 304(5669):452–454.
- Samejima K, Ueda Y, Doya K, Kimura M (2005) Representation of action-specific reward values in the striatum. *Science* 310(5752):1337–1340.
- Wang AY, Miura K, Uchida N (2013) The dorsomedial striatum encodes net expected return, critical for energizing performance vigor. *Nat Neurosci* 16(5): 639–647.
- Parent M, Lévesque M, Parent A (2001) Two types of projection neurons in the internal pallidum of primates: Single-axon tracing and three-dimensional reconstruction. *J Comp Neurol* 439(2):162–175.
- Rajakumar N, Elisevich K, Flumerfelt BA (1993) Compartmental origin of the striato-entopeduncular projection in the rat. *J Comp Neurol* 331(2):286–296.
- Stephenson-Jones M, Samuelsson E, Ericsson J, Robertson B, Grillner S (2011) Evolutionary conservation of the basal ganglia as a common vertebrate mechanism for action selection. *Curr Biol* 21(13):1081–1091.
- Stephenson-Jones M, Floros O, Robertson B, Grillner S (2012) Evolutionary conservation of the habenular nuclei and their circuitry controlling the dopamine and 5-hydroxytryptophan (5-HT) systems. *Proc Natl Acad Sci USA* 109(3):E164–E173.
- Bromberg-Martin ES, Matsumoto M, Hong S, Hikosaka O (2010) A pallidus-habenula-dopamine pathway signals inferred stimulus values. *J Neurophysiol* 104(2):1068–1076.
- Hong S, Hikosaka O (2008) The globus pallidus sends reward-related signals to the lateral habenula. *Neuron* 60(4):720–729.
- Matsumoto M, Hikosaka O (2007) Lateral habenula as a source of negative reward signals in dopamine neurons. *Nature* 447(7148):1111–1115.
- Shabel SJ, Proulx CD, Trias A, Murphy RT, Malinow R (2012) Input to the lateral habenula from the basal ganglia is excitatory, aversive, and suppressed by serotonin. *Neuron* 74(3):475–481.
- Stamatakis AM, Stuber GD (2012) Activation of lateral habenula inputs to the ventral midbrain promotes behavioral avoidance. *Nat Neurosci* 15(8):1105–1107.

18. Ménard A, Auclair F, Bourcier-Lucas C, Grillner S, Dubuc R (2007) Descending GABAergic projections to the mesencephalic locomotor region in the lamprey *Petromyzon marinus*. *J Comp Neurol* 501(2):260–273.
19. Robertson B, Saitoh K, Ménard A, Grillner S (2006) Afferents of the lamprey optic tectum with special reference to the GABA input: Combined tracing and immunohistochemical study. *J Comp Neurol* 499(1):106–119.
20. Stephenson-Jones M, Ericsson J, Robertson B, Grillner S (2012) Evolution of the basal ganglia: Dual-output pathways conserved throughout vertebrate phylogeny. *J Comp Neurol* 520(13):2957–2973.
21. Gerfen CR (1992) The neostriatal mosaic: Multiple levels of compartmental organization. *J Neural Transm Suppl* 36(Suppl. 36):43–59.
22. Graybiel AM (1990) Neurotransmitters and neuromodulators in the basal ganglia. *Trends Neurosci* 13(7):244–254.
23. Graybiel AM, Ragsdale CW, Jr. (1978) Histochemically distinct compartments in the striatum of human, monkeys, and cat demonstrated by acetylthiocholinesterase staining. *Proc Natl Acad Sci USA* 75(11):5723–5726.
24. Fujiyama F, et al. (2011) Exclusive and common targets of neostriatofugal projections of rat striosome neurons: A single neuron-tracing study using a viral vector. *Eur J Neurosci* 33(4):668–677.
25. Robertson B, et al. (2012) The dopamine D2 receptor gene in lamprey, its expression in the striatum and cellular effects of D2 receptor activation. *PLoS ONE* 7(4):e35642.
26. Hikosaka O (2010) The habenula: From stress evasion to value-based decision-making. *Nat Rev Neurosci* 11(7):503–513.
27. Ji H, Shepard PD (2007) Lateral habenula stimulation inhibits rat midbrain dopamine neurons through a GABA(A) receptor-mediated mechanism. *J Neurosci* 27(26):6923–6930.
28. Leichnetz GR, Astruc J (1977) The course of some prefrontal corticofugals to the pallidum, substantia innominata, and amygdaloid complex in monkeys. *Exp Neurol* 54(1):104–109.
29. Mettler FA (1935) Corticofugal fiber connections of the cortex of macaca mullatta. The frontal region. *J Comp Neurol* 61(3):509–542.
30. Naito A, Kita H (1994) The cortico-pallidal projection in the rat: An anterograde tracing study with biotinylated dextran amine. *Brain Res* 653(1-2):251–257.
31. Cardinal RN, Parkinson JA, Hall J, Everitt BJ (2002) Emotion and motivation: The role of the amygdala, ventral striatum, and prefrontal cortex. *Neurosci Biobehav Rev* 26(3):321–352.
32. Wallis JD (2012) Cross-species studies of orbitofrontal cortex and value-based decision-making. *Nat Neurosci* 15(1):13–19.
33. Amemori K, Graybiel AM (2012) Localized microstimulation of primate pregenual cingulate cortex induces negative decision-making. *Nat Neurosci* 15(5):776–785.
34. Alexander GE, Crutcher MD (1990) Functional architecture of basal ganglia circuits: Neural substrates of parallel processing. *Trends Neurosci* 13(7):266–271.
35. Hammond C, Shibasaki T, Rouzaire-Dubois B (1983) Branched output neurons of the rat subthalamic nucleus: Electrophysiological study of the synaptic effects on identified cells in the two main target nuclei, the entopeduncular nucleus and the substantia nigra. *Neuroscience* 9(3):511–520.
36. Larsen KD, Sutin J (1978) Output organization of the feline entopeduncular and subthalamic nuclei. *Brain Res* 157(1):21–31.
37. Nakanishi H, Kita H, Kitai ST (1990) Intracellular study of rat entopeduncular nucleus neurons in an in vitro slice preparation: Electrical membrane properties. *Brain Res* 527(1):81–88.
38. Robledo P, Vezole I, Feger J (1988) Excitatory effect of subthalamo-nigral and subthalamo-pallidal efferent pathways in the rat. *C R Acad Sci III* 307(3):133–138.
39. Amemori K, Gibb LG, Graybiel AM (2011) Shifting responsibly: The importance of striatal modularity to reinforcement learning in uncertain environments. *Front Hum Neurosci* 5:47.
40. White NM, Hiroi N (1998) Preferential localization of self-stimulation sites in striosomes/patches in the rat striatum. *Proc Natl Acad Sci USA* 95(11):6486–6491.
41. Christoph GR, Leonzio RJ, Wilcox KS (1986) Stimulation of the lateral habenula inhibits dopamine-containing neurons in the substantia nigra and ventral tegmental area of the rat. *J Neurosci* 6(3):613–619.
42. Hong S, Zhou TC, Smith M, Saleem KS, Hikosaka O (2011) Negative reward signals from the lateral habenula to dopamine neurons are mediated by rostromedial tegmental nucleus in primates. *J Neurosci* 31(32):11457–11471.
43. Weiner DM, et al. (1991) D1 and D2 dopamine receptor mRNA in rat brain. *Proc Natl Acad Sci USA* 88(5):1859–1863.
44. Fillion M, Tremblay L, Bédard PJ (1991) Effects of dopamine agonists on the spontaneous activity of globus pallidus neurons in monkeys with MPTP-induced parkinsonism. *Brain Res* 547(1):152–161.
45. Napier TC, Simson PE, Givens BS (1991) Dopamine electrophysiology of ventral pallidal/substantia innominata neurons: Comparison with the dorsal globus pallidus. *J Pharmacol Exp Ther* 258(1):249–262.
46. Lavoie B, Smith Y, Parent A (1989) Dopaminergic innervation of the basal ganglia in the squirrel monkey as revealed by tyrosine hydroxylase immunohistochemistry. *J Comp Neurol* 289(1):36–52.
47. Araki M, McGeer PL, McGeer EG (1984) Retrograde HRP tracing combined with a pharmacohistochemical method for GABA transaminase for the identification of presumptive GABAergic projections to the habenula. *Brain Res* 304(2):271–277.
48. Institute of Laboratory Animal Research; National Research Council (1996) *The Guide for the Care and Use of Laboratory Animals* (National Academy Press, Washington, DC).
49. Venables WN, Ripley BD (2002) Univariate statistics. In *Modern Applied Statistics with S*. (Springer), pp 126–133.
50. Ericsson J, et al. (2013) Evolutionarily conserved differences in pallial and thalamic short-term synaptic plasticity in striatum. *J Physiol* 591(Pt 4):859–874.